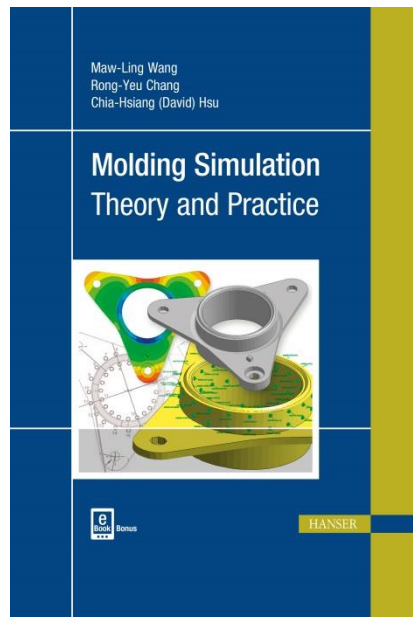


HANSER



Sample Pages

Molding Simulation: Theory and Practice

Maw-Ling Wang
Rong-Yeu Chang
Chia-Hsiang (David) Hsu

ISBN (Book): 978-1-56990-619-4

ISBN (E-Book): 978-1-56990-620-0

For further information and order see

www.hanserpublications.com (in the Americas)

www.hanser-fachbuch.de (outside the Americas)

© Carl Hanser Verlag, München

Contents

Acknowledgments	V
Preface	VII
1 Overview of Plastics Molding	1
1.1 Introduction to Injection Molding	1
1.1.1 The Systems of Injection Molding	3
1.1.1.1 The Cycle of Injection Molding	3
1.1.1.2 Injection Machine	4
1.1.2 Defects of Injection Molded Products	8
1.1.2.1 Short Shot	9
1.1.2.2 Warp	9
1.1.2.3 Flash	10
1.1.2.4 Sink Mark or Void	11
1.1.2.5 Air Trap	11
1.1.2.6 Burn Mark	12
1.1.2.7 Delamination	12
1.1.2.8 Fish Eye	12
1.1.2.9 Flow Mark	13
1.1.2.10 Stress Mark	13
1.1.2.11 Hesitation	14
1.1.2.12 Jetting	14
1.1.2.13 Splays	14
1.1.2.14 Weld Line	15
1.2 Core Values of Molding Simulation	16
1.2.1 Application of CAE Technology in Injection Molding	16

2	Material Properties of Plastics	19
2.1	Overview	19
2.2	Rheological Properties	21
2.2.1	Viscosity	22
2.2.1.1	Effects of Non-Newtonian and Molecular Conformation	22
2.2.1.2	Effects of Shear Rate	24
2.2.1.3	Effects of Temperature	26
2.2.1.4	Effects of Pressure	27
2.2.1.5	Theoretical Models	27
2.2.2	Viscoelastic Fluids	29
2.2.2.1	Viscoelastic Behavior	29
2.2.2.2	Theoretical Models	31
2.3	Thermodynamic and Thermal Properties	35
2.3.1	Specific Heat Capacity	35
2.3.1.1	Theoretical Models	36
2.3.2	Melting Point and Glass Transition Temperatures	38
2.3.3	PVT Equation of State	39
2.3.3.1	Definition	39
2.3.3.2	Theoretical Models	39
2.3.3.3	Effects of Non-equilibrium State on PVT	42
2.3.4	Thermal Conductivity and Heat Transfer Coefficient	43
2.3.4.1	Definition	43
2.3.4.2	Theoretical Models	43
2.3.4.3	Mold-Melt Contact and Heat Transfer Coefficient (HTC)	44
2.3.4.4	The Heat Transfer Coefficient (HTC)	44
2.4	Mechanical Properties	45
2.4.1	Stress and Strain of Plastics	45
2.4.2	Solid Viscoelasticity	45
2.4.3	Theoretical Model	46
2.5	Kinetic Properties	47
2.5.1	Crystalline	47
2.5.2	Theoretical Models	48
2.5.3	Effects of Cooling Rate on Crystallization	49
2.6	Curing Kinetics	50
2.6.1	Curing Phenomenon	50
2.6.2	Theoretical Models	51
2.6.3	Curing Effect on Viscosity	52
2.7	References	54

3	Part and Mold Design	55
3.1	Part Design	55
3.1.1	Golden Rule: Uniform Wall Thickness	55
3.1.2	Wall Thickness versus Flow Length	58
3.1.3	Radius/Fillets and Chamfer Angle	60
3.1.4	Rib and Boss	61
3.1.5	Draft Angle	66
3.1.6	Design for Manufacturing (DFM)	66
3.1.7	Summary	68
3.2	Mold Design	68
3.2.1	Basics	69
3.2.2	Gate Design	72
3.2.2.1	Gate Number	72
3.2.2.2	Gate Location	73
3.2.2.3	Gate Types	76
3.2.3	Runner Design	79
3.2.3.1	Runner Shape and Dimension	80
3.2.3.2	Multi-Cavity Runner Design	81
3.2.4	Cooling Design	82
3.2.5	Others	83
3.2.5.1	Ejector System	83
3.2.5.2	Venting Design	84
3.3	References	85
4	Process Conditions	87
4.1	Introduction of Injection Molding Cycle	87
4.1.1	Brief Introduction to Injection Molding Machine Units	87
4.1.2	Injection Molding Cycle	89
4.1.3	Molding Window	92
4.1.4	PVT Variations during Injection Stages	93
4.2	Plasticizing Conditions	103
4.2.1	Nozzle Temperature and Cylinder Temperatures	103
4.2.2	Back Pressure, Screw rpm, Suck Back, and Metering Stroke	105
4.3	Filling Conditions	110
4.3.1	Filling Time versus Injection Velocity	110
4.3.2	Injection Pressure	112
4.3.3	VP Switch	115
4.4	Packing Conditions	117
4.4.1	Packing Time and Packing Pressure	117

4.5	Cooling Conditions	119
4.5.1	Cooling Time	119
4.5.2	Coolant Flow Rate	119
4.5.3	Mold Temperature	120
5	Molding Simulation Methodology	123
5.1	The Goal of Molding Simulation	123
5.1.1	Design Verification and Optimization	124
5.1.1.1	Overview of Design for Manufacture (DFM)	124
5.1.1.2	CAE and DFM: A Practical Case Study	126
5.1.2	Process Conditions Optimization	133
5.1.2.1	Molding Stability	133
5.1.2.2	Real Case	135
5.2	Basics of Simulation Equations	139
5.2.1	Governing Equations	139
5.2.2	Numerical Approximation	141
5.2.2.1	Finite Difference Method (FDM)	141
5.2.2.2	Finite Volume Method (FVM)	144
5.2.2.3	Finite Element Method (FEM)	147
5.3	What is Molding Simulation?	149
5.3.1	Brief History of Molding Simulation	149
5.3.2	Simulation Workflow	155
5.4	References	158
6	Flow Consideration versus Part Features	159
6.1	Basics	159
6.1.1	Flow Behavior of Plastic Melt in the Cavity	159
6.1.2	Effects of Filling Time	164
6.1.3	Flow Rate versus Injection Pressure	165
6.1.3.1	Flow Rate Curve Setting	165
6.1.3.2	Relationship of Injection Rate and Injection Pressure	169
6.1.4	VP Switch and Cavity Pressure	175
6.1.5	Effects of Part Thickness	184
6.1.6	Material Viscosity and Flow Behavior	188
6.1.7	Summary	192
6.2	Practical Applications	193
6.2.1	CAE Solution to Stress Mark in a Phone Shell	193
6.2.2	Flow Rate Effect on Injection Pressure of Laptop Product	196
6.3	CAE Case Study	198
6.4	References	201

7	Runner and Gate Design	203
7.1	Basics	203
7.1.1	General Design Guide of Runners	203
7.1.2	General Design Guide of Gates	207
7.1.3	Gate Sealing	216
7.1.4	Flow Balance	218
7.2	Practical Applications	225
7.2.1	CAE Verification on MeltFlipper® Design	225
7.2.2	CAE Verification of Multi-Cavity Systems	231
7.3	CAE Case Study	234
7.4	References	236
8	Cooling Optimization	237
8.1	Basics	237
8.1.1	Heat Transfer Mechanism	238
8.1.2	Design Golden Rule: Uniform Mold Temperature	241
8.1.3	General Design Guide of Cooling Channel	245
8.1.4	Cooling Efficiency: Coolant Flow Consideration	249
8.1.5	Cooling Time Estimate	252
8.1.6	Use CAE Cooling Analysis	254
8.1.7	Conformal Cooling Application	258
8.2	Practical Applications	262
8.2.1	Digital Camera Cover	262
8.2.2	Cartridge	267
8.3	CAE Case Study	270
9	Warpage Control	273
9.1	Basics	273
9.1.1	The Causes of Warpage	276
9.1.2	Material Effects	278
9.1.3	Geometrical Effects	282
9.1.4	Process Condition Effects	284
9.1.5	Criteria of CAE Warp Analysis	285
9.1.6	Methods to Minimize Warpage	290
9.2	Practical Applications	295
9.2.1	CAE Solution on Warpage of Connector	295
9.3	CAE Case Study	301

10	Fiber Orientation Control	303
10.1	Basics	304
10.1.1	Process Principle	306
10.1.2	Theory Models	307
10.1.3	Advantages and Challenges	316
10.2	Practical Applications	317
10.3	CAE Case Study	321
10.4	References	322
11	Hot Runner Optimization	325
11.1	Basics	325
11.1.1	Process Principle	326
11.1.2	Temperature Control in a Hot Runner System	330
11.1.3	Advantages and Challenges	332
11.2	Practical Applications	341
11.2.1	CAE Verification on a Single-Gate Hot Runner System	341
11.2.2	CAE Pin Movement Control of Valve Gate	349
11.3	CAE Case Study	353
12	Co-/Bi-Injection Molding	357
12.1	Basics	358
12.1.1	Process Principle	358
12.1.2	Advantages and Challenges	361
12.1.3	Theory Models	363
12.2	Practical Applications	364
12.2.1	Co-Injection Molding of Fork Model	364
12.2.2	Co-Injection Molding: Core Breakthrough and Flow Imbalance	366
12.2.3	CAE Case of Bi-Injection Molding	370
12.3	CAE Case Study	374
12.4	References	376
13	Gas-/Water-Assisted Injection Molding	377
13.1	Basics	377
13.1.1	Process Principle	378
13.1.1.1	Short-Shot Process	379
13.1.1.2	Full-Shot Process	380
13.1.2	Advantages and Challenges	381

13.2 Practical Applications	389
13.2.1 CAE Verification on GAIM	390
13.2.2 CAE Verification on WAIM	393
13.2.3 CAE Verification on GAIM: Fingering Effect	395
13.3 CAE Case Study	398
13.4 References	400
14 Foam Injection Molding	401
14.1 Basics	401
14.1.1 Microcellular Process Principle	402
14.1.2 Advantages and Challenges	405
14.1.3 Theory Models	406
14.2 Practical Applications	409
14.2.1 CAE Verification on Microcellular Injection Molding	409
14.2.2 CAE Verification on Chemical Foaming Injection Molding	417
14.2.3 Summary	420
14.3 CAE Case Study	420
14.4 References	422
15 Powder Injection Molding	425
15.1 Basics	425
15.1.1 Process Principle	426
15.1.2 Advantages and Challenges	427
15.1.3 Theory Models	430
15.2 Practical Applications	435
15.2.1 CAE Verification on an Electronic Device	435
15.3 CAE Case Study	438
15.4 References	439
16 Resin Transfer Molding	441
16.1 Basics	441
16.1.1 Process Principle	445
16.1.2 Advantages and Challenges	448
16.2 Theoretical Models	450
16.2.1 2.5D Analysis	450
16.2.2 3D Analysis	452
16.2.3 Measurement of Permeability	454
16.2.4 Porosity	456

16.2.5 Measurement of Chemorheological Properties	457
16.2.6 Simulation Parameters	458
16.3 Practical Applications	458
16.3.1 CAE Verification on Edge Effects	458
16.3.2 CAE Verification on Thickness-Direction Flow	461
16.3.3 CAE Verification on a Wind Turbine Blade	465
16.3.4 CAE Verification on Mat Effects	467
16.3.5 CAE Verification on Flybridge	469
16.4 CAE Case Study	473
16.5 References	474
17 Integrated Circuit Packaging	475
17.1 Basics	475
17.1.1 Process Principle	480
17.1.2 Advantages and Challenges	483
17.1.3 Theoretical Models	485
17.2 Practical Applications	489
17.2.1 CAE Verification on Void Prediction	489
17.2.2 Fluid-Structure Interactions: Wire Sweep Analysis	493
17.2.3 Fluid-Structure Interactions: Paddle Shift and Chip Deformation Analysis	495
17.2.4 Warpage Prediction of In-Mold/Post-Mold Process	502
17.3 CAE Case Study	505
17.4 References	507
Index	509

Acknowledgments

We would like to thank and acknowledge Beaumont Technologies, Inc. for the flow imbalance case in Section 7.1.4 and Section 7.2.1, OPM Laboratory Co., Ltd. for the conventional and conformal cooling design cases in Section 8.2.1, Ann Tong Industrial Co., Ltd. for the single-gate hot runner system case in Section 11.2.1, Prof. Shi-Chang Tseng and Prof. Shia-Chung Chen for the gas-assisted injection molding cases in Section 13.2.1 and Section 13.2.3, respectively, Prof. Shih-Jung Liu for the water-assisted injection molding case in Section 13.2.2, Trexel Inc. for the MuCell® case in Section 14.2.1, Prof. Shyh-Shin Hwang for the chemical foaming injection molding case in Section 14.2.2, Prof. Shun-Tian Lin for the metal injection molding case in Section 15.2.1, Atech Composites Co., Ltd. for resin transfer molding cases in Section 16.3.3 and Section 16.3.5, Associate Prof. Yuan Yao for the resin transfer molding case in Section 16.3.4, and Amkor Technology Korea Inc. for the IC packaging cases in Section 17.2.1 and Section 17.2.2. These practical cases are quite valuable and helpful to illustrate how to co-develop innovative molding technologies and solve molding issues with the CAE tool.

We would also like to thank the following for their contributions: Dr. Che-Ping (Barton) Lin on Chapter 1, Dr. Chen-Chieh (Jye) Wang and Dr. Chih-Wei (Joe) Wang on Chapter 2, Tsai-Hsin (Sam) Hsieh, Tsai-Heng (Paul) Tsai, and Dr. Ying-Mei (May) Tsai on Chapter 3, Tsai-Hsin (Sam) Hsieh, Wen-Bing (Webin) Liu, and Dr. Ying-Mei (May) Tsai on Chapter 4, Hsien-Sen (Ethan) Chiu and Dr. Ying-Mei (May) Tsai on Chapter 5, Yu-Chih (Goran) Liu and Wen-Bing (Webin) Liu on Chapter 6, Dr. Che-Ping (Barton) Lin and Dr. Sung-Wei (Franz) Huang on Chapter 7, Dr. Chih-Wei (Joe) Wang and Dr. Sung-Wei (Franz) Huang on Chapter 8, Dr. Shih-Po (Tober) Sun on Chapter 9, Dr. Huan-Chang (Ivor) Tseng on Chapter 10 and Chapter 15, Tsai-Hsin (Sam) Hsieh on Chapter 11, Dr. Chih-Chung (Jim) Hsu on Chapter 12, Chapter 13, and Chapter 17, Yuan-Jung (Dan) Chang on Chapter 14, and Hsun (Fred) Yang on Chapter 16. They dedicated their wisdom and skills, and a great deal of time, to complete this wonderful book.

Moreover, a very special thanks to Chia-Lin (Carol) Li for redrawing figures, Pao-Hui (Ryan) Wan for his assistive editing, and Dr. Ying-Mei (May) Tsai and Dr. Che-Ping (Barton) Lin for their executive editing.

Preface

Injection molding techniques have been developed over decades and well-applied in automotive, 3C (Computer, Communication, and Consumer electronics), optics, medical products, and in daily necessities, among other areas. Due to this long-term development and widely ranging applications, the individual molding criteria have been specialized in several industries to fit various product specifications and innovative materials.

Many industries are producing novel plastic products, such as FRPs (fiber reinforced plastics) replacing metal to reduce weight while maintaining the structural strength of automotive parts. The unique appearance achievable from techniques such as multi-component design of 3C products is more attractive than that from the common design by conventional injection molding. The high turnover rate in mobile products has raised the demand for plastic lenses so that the capacity and profits of the optics industry are ensured as long as production stability of high-precision-shaped lenses can be achieved in multi-cavity molding. Usually, medical plastic products have a high added value, but they especially must pass severe material certification standards at the primary stage, and dust-free or sterile production may be necessary. As for daily necessities, although part dimensional precision is not demanded as much as in other industries, there are still molding issues to consider; for example, conformal cooling method might be evaluated in order to reduce the cycle time.

The increasing requirements and diversity of plastic products demand a shorter time to market. However, much time can be spent in developing the procedures for some products, from concept generation, design drawing, mold tooling and assembling, trial-molding to mass production. “How can the procedures be shortened using CAE (Computer Aided Engineering) tools?” then becomes a key question for industry. The idea is to predict potential molding problems and defects by CAE during the design stage, modify the design according to these results, and then re-analyze until the best design is obtained. Since the 1970s, virtual trial moldings have been implemented by computer using injection molding simulation CAE tools to check whether the molding parameters are good enough for manufacture. These

parameters are part design, gate design, runner layout, cooling layout, molding materials, process conditions, and so on. From CAE, the optimized parameters can be estimated efficiently and provided as the initial-guess settings for the real molding to cost down in time, manpower, material, and energy. To summarize, CAE is a decades-proven design-verification tool for real applications of the injection molding process.

In addition to conventional injection molding, there are many innovative molding processes that have appeared. Characteristics of lightweight parts, low clamping force, and low shrinkage are noted in the G/WAIM (Gas-/Water-Assisted Injection Molding) and MuCell® processes. With co-/bi-injection, multi-component or multi-functional parts can be produced by one-shot molding. The compression operation of ICM (Injection Compression Molding) provides a uniform packing mechanism on a plastic melt that compensates the non-homogeneous packing of injection molding. Metal or ceramic PIM (Powder Injection Molding) is especially adapted to manufacture the green part of highly precise and complicated geometry products. When using a hot runner system, the most important thing is accurate temperature control. Moreover, improvements in plastics molding techniques are not only exhibited in injection processes, but also, for example, in consideration of the resin curing reaction within the multi-substrate molding of an IC package, a process that has evolved greatly.

Molding issues become more challenging and complicated with innovations in processes and materials, which can lead to a longer time and higher cost in conditions optimization. In particular, when fiber composites are involved, obtaining favorable fiber orientations and maintaining longer fiber lengths after processing are extremely important goals, because the microstructures of the materials dominate the product quality. In RTM (Resin Transfer Molding), the microstructures are related to the resin impregnation degree inside the continuous fiber mat or woven roving. The involvement of the effects of surface tension, fiber deformation, and resin curing reaction all make RTM process control more difficult. Fortunately, CAE is nowadays available to simulate these new procedures and as a process innovation tool.

From decades of experience in CAE assistance in molding troubleshooting, we have found that processing knowledge is as important as software operation to CAE users. To make a high-quality molded product, the total effects of part design, mold design and manufacture, machine capability, and material properties must all be taken into account and then integrated into the CAE tool to implement design verification and conditions optimization wisely. Each of these definitely involves a deep knowledge, whether in theory and/or empirical formula. When talking about molding issues, plastics rheology and the designs of part and mold are especially the key criteria since their interactions will dominate the material property variations inside the mold.

At Moldex3D, as worldwide leaders in molding simulation software, we are not just continuously enhancing CAE capability but also intend to help industry people improve their molding-related abilities. The importance of training and instruction has become strongly apparent to us. As a result, this book consists of plastics molding theory, practical applications, and case studies intended to elaborate the molding system and melt flowing behaviors in an easy-to-understand way. The practical examples show how to use CAE to achieve design verification and process innovation in conventional injection molding, G/WAIM, co-/bi-injection, foam injection molding, PIM, RTM, and IC packaging. With this book, readers can effectively learn molding simulation applications and its importance in molding industries.

The CAE case study exercises found in the book for execution in the Moldex3D software can be downloaded from the Website: <https://moldex3d.box.com/s/zr6fvc1vlhbi4ocx111jwd3wmxt4ooif>, for which the QR code is as follows:



Maw-Ling Wang

Rong-Yeu Chang

Chia-Hsiang (David) Hsu

Table 6.2 Polymer Type versus Clamping Force [3] (*continued*)

Resin	tonnes/in ²	tonnes/cm ²	MN/m ²
AS (SAN) (long flows)	3.0–4.0	0.465–0.62	46.3–61.8
LDPE	1.0–2.0	0.155–0.31	15.4–30.9
HDPE	1.5–2.5	0.233–0.388	23.2–38.6
HDPE (long flows)	2.5–3.5	0.388–0.543	38.6–54.0
PP (Homo/Copolymer)	1.5–2.5	0.233–0.388	23.3–38.6
PP (H/Co) (long flows)	2.5–3.5	0.388–0.543	38.6–54.0
PPVC	1.5–2.5	0.233–0.388	23.3–38.6
UPVC	2.0–3.0	0.31–0.465	30.9–46.3
PA6, PA66	4.0–5.0	0.62–0.775	61.8–77.2
PMMA	2.0–4.0	0.31–0.62	30.9–61.8
PC	3.0–5.0	0.465–0.775	46.3–77.2
POM (Homo/Copolymer)	3.0–5.0	0.465–0.775	46.3–77.2
PET (Amorphous)	2.0–2.5	0.31–0.388	30.9–38.6
PET (Crystalline)	4.0–6.0	0.62–0.93	61.8–92.6
PBT	3.0–4.0	0.465–0.62	46.3–61.8
CA	1.0–2.0	0.155–0.31	15.4–30.9
PPO-M (unreinforced)	2.0–3.0	0.31–0.465	30.9–46.3
PPO-M (reinforced)	4.0–5.0	0.62–0.775	61.8–77.2
PPS	2.0–3.0	0.31–0.465	30.9–46.3

6.1.6 Material Viscosity and Flow Behavior

The basic principle for setting the injection speed and pressure in the filling stage is that high speed and high pressure facilitate the filling to be finished in a short time to avoid fast cooling of the melt, which would increase the flow resistance. The reason for using a high pressure is to avoid a drop of injection speed due to insufficient injection pressure, which may lead to deviation from the original parameter setting.

When the plastic material is flowing, an internal pressure (counteractive force) is generated by the flow resistance as the plastic is compressed. A faster pressure rise denotes a higher flow resistance, and thus the pressure loss from flowing through the part becomes higher. By increasing the melt temperature to reduce the viscosity of the material, the flow resistance can be reduced, and a lower flow resistance in the filling stage leads to a smaller increase of the internal pressure.

Possible causes for a rising flow resistance, leading to high internal pressure and high pressure loss, are as follows: thinner thickness, long flowing distance, lower mold/melt temperature, slower injection speed, and high viscosity.

Because the flow resistance is proportional to the melt viscosity, it is still possible to change the viscosity and reduce the flow resistance in the same mold and same material through modification of the molding conditions. Polymer materials are non-Newtonian fluids and hence their viscosity not only changes at different temperatures but also depends on the shear rate.

To understand the influence of the shear rate on the viscosity of a plastic material, it is necessary to interpret the implication of a viscosity curve of material. The viscosity affects the flow resistance, and then the filling pressure, as well as the specifications and capacity of machine required. The viscosity difference of the plastic material between each region in the mold cavity also affects the pressure transmission, the flow balance, and the follow-up packing pressure transmission, which has a direct relationship to the mass and quality of the part.

Therefore, the quality control of the part is an important factor to understand the relationship between viscosity variation and molding conditions of plastic materials. The viscosity variation of polystyrene (PS) is shown as an example in Figure 6.36.

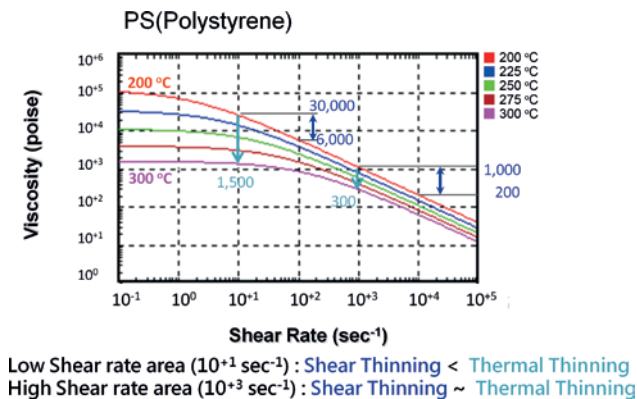


Figure 6.36 Viscosity of polystyrene

In the low shear rate zone where the shear rate is $1.0 \times 10^1 \text{ sec}^{-1}$ and the temperature is $200 \text{ }^\circ\text{C}$, by increasing the temperature from 200 to 300 o, the viscosity is reduced from 30,000 poise to 1500 poise. By increasing the shear rate from $1.0 \times 10^1 \text{ sec}^{-1}$ to $1.0 \times 10^2 \text{ sec}^{-1}$, the viscosity can be reduced from 30,000 poise to 6000 poise. Therefore, the influence of the shear rate on the viscosity is relatively smaller than the influence of the temperature.

In the high shear rate zone where the shear rate is $1.0 \times 10^3 \text{ sec}^{-1}$ and the temperature is $200 \text{ }^\circ\text{C}$, by increasing the temperature from 200 to $300 \text{ }^\circ\text{C}$, the viscosity is reduced from 1000 poise to 300 poise. By increasing the shear rate from $1.0 \times 10^3 \text{ sec}^{-1}$ to $1.0 \times 10^4 \text{ sec}^{-1}$, the viscosity can be reduced from 1000 poise to

200 poise. Therefore, the influence of the shear rate on the viscosity is close to but slightly larger than the influence of the temperature on the viscosity.

Regarding various effects of viscosity, the viscosity curves of three different groups of plastic materials are compared in Figure 6.37 to explore the sensitivity of viscosity versus temperature and shear rate.

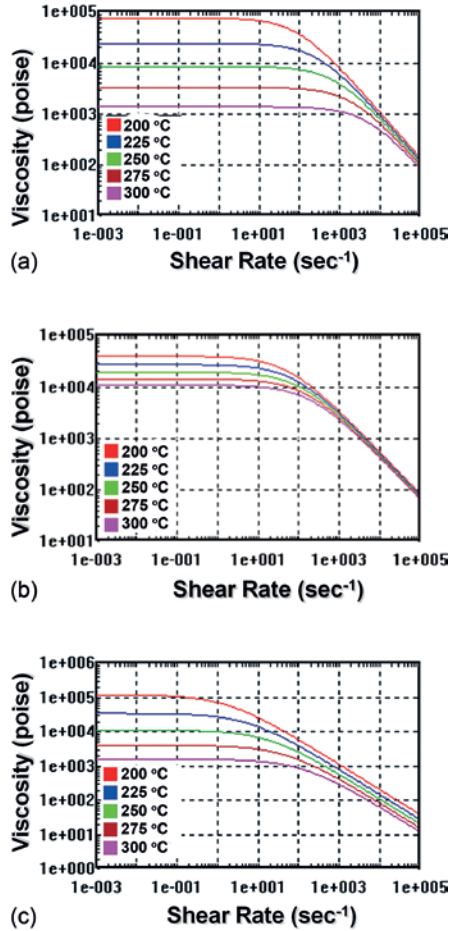


Figure 6.37 Viscosity: (a) temperature sensitive, (b) shear rate sensitive, and (c) temperature and shear rate sensitive

Figure 6.37(a) shows a bigger gap between each temperature curve, indicating a significant effect on decreasing the viscosity by raising the temperature but an insignificant effect on decreasing the viscosity by raising the shear rate, which shows that the viscosity of the material is sensitive to temperature. Figure 6.37(b) shows a smaller gap between each temperature curve, indicating an insignificant effect on decreasing the viscosity by raising the temperature but a significant effect on

decreasing the viscosity by raising the shear rate, which shows that the viscosity of the material is sensitive to shear rate. Figure 6.37(c) shows a bigger gap between each temperature curve and also the decrease of viscosity with the increase of shear rate is significant, which shows that the viscosity of the material is sensitive to both temperature and shear rate.

Figure 6.38 shows a comparison of the injection pressure under different melt temperatures (250 and 280 °C) for polymethylmethacrylate (PMMA). As the melt temperature rises, the viscosity of the material drops and thus leads to a decrease of the flow resistance as well as the injection pressure. When the melt temperature is 250 °C and the filling time is 1.0 sec, the injection pressure reaches 100 MPa; when the melt temperature is 280 °C and the filling time is 1.0 sec, the injection pressure reaches 70 MPa.

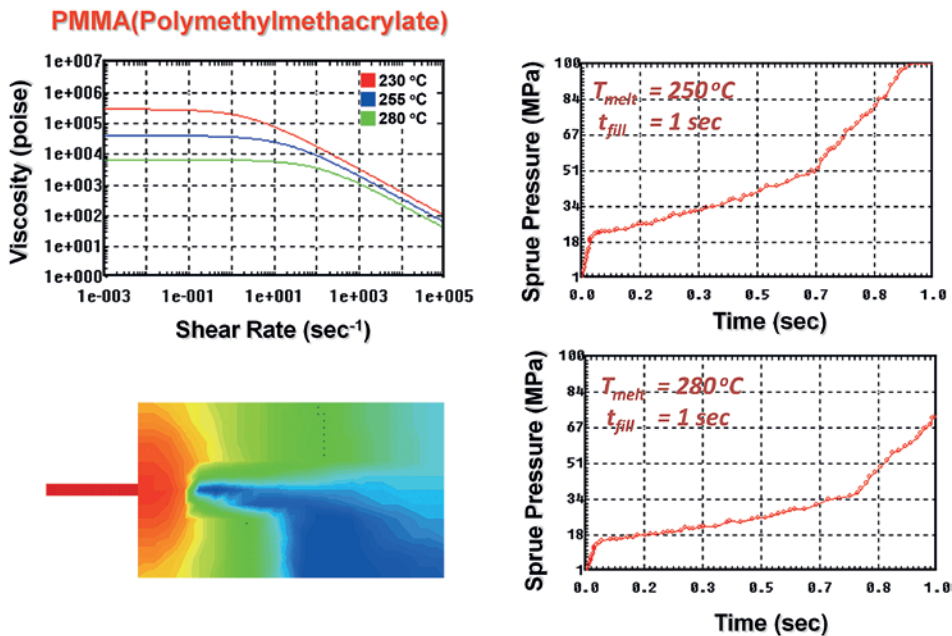


Figure 6.38 Melt temperature versus injection pressure

Different materials have different viscous characteristics. The influence on the injection pressure of three different plastic materials is compared in Figure 6.39. By setting the same filling time at 1.0 sec, the injection pressure for polypropylene (PP) is 32 MPa, and 28 MPa for polystyrene (PS), whereas polymethylmethacrylate (PMMA) requires 100 MPa to complete the filling process. Furthermore, when the filling time reaches 0.8 sec for PMMA, the pressure already hits the upper limit of 100 MPa, which indicates that the pressure control mode already kicks in and the system cannot maintain the original fixed flow rate for filling.

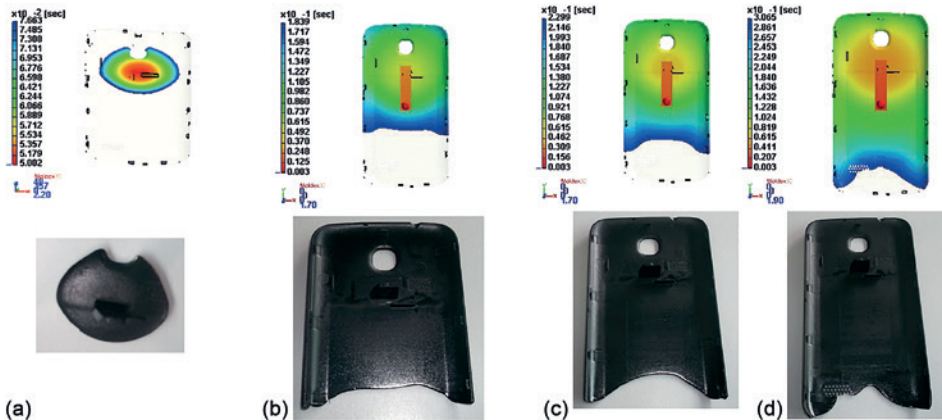


Figure 6.42 Consistency between CAE analysis and experiment in melt front time

The surface quality of an actual part can also be assessed through an analysis result. For example, by observing the surface quality of the injection-molded part as shown in Figure 6.43, a significant mark defect is seen at the boundary between the thickness of 0.7 mm and 1.0 mm in the center, where a considerable shear stress difference also exists.

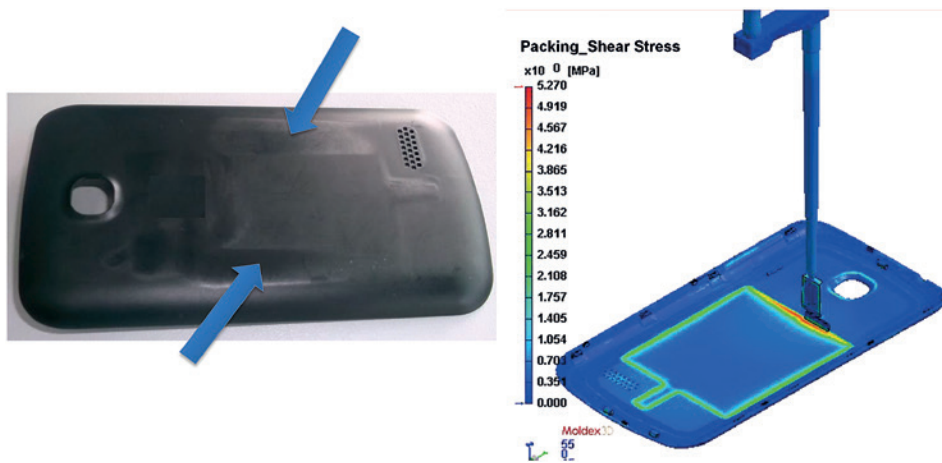


Figure 6.43 Mark defect versus shear stress

As shown in Figure 6.44, the surface quality of the part can be improved by changing the thickness of the design. Figure 6.44(a) is the original design and Figure 6.44(b) is the revised one. The main change is to design a smooth thickness transition area at the boundary where the thickness of 0.7 mm and 1.0 mm meet.

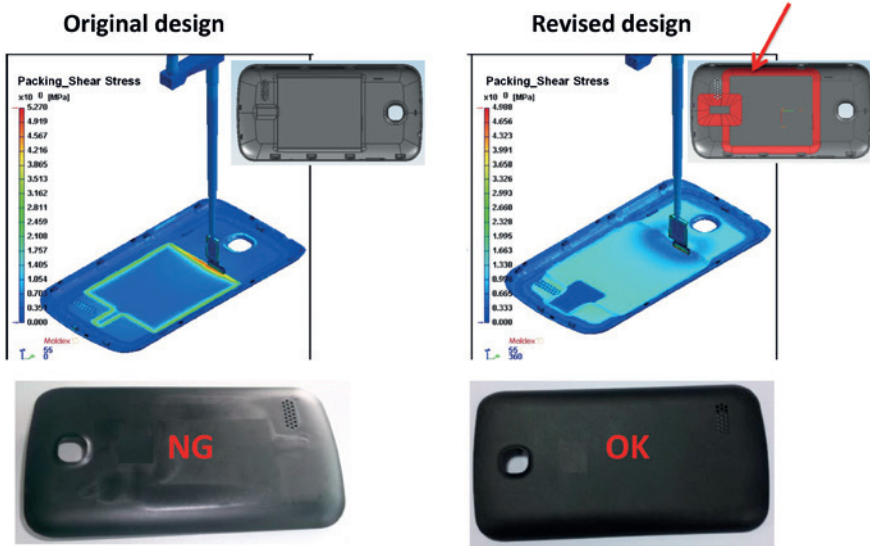


Figure 6.44 Broaden the thickness transition area

From the packing result of shear stress distribution analyzed by CAE as well as the picture showing the part surface, the frame-shaped distribution of shear stress in the central area no longer exists, and the actual surface quality of the part is indeed significantly improved.

6.2.2 Flow Rate Effect on Injection Pressure of Laptop Product

Concerning the injection stroke setting, the runner stroke and the mold cavity stroke are calculated respectively. The runner stroke can be converted from the runner volume, and the mold cavity stroke can be estimated by using 60–90% of the mold cavity volume. Figure 6.45 shows an example using Moldex3D to describe how a multi-step flow rate setting is configured (reference example). The specifications are listed as follows:

Part model: D part of a laptop PC (bottom plate)

Part volume: 122.16 cm³

Part dimensions: 315 mm × 225 mm × 20 mm

Main thickness: 2 mm

Material: PC/ABS

Runner system: hot runner

Capacity of injection molding machine: 450 tons

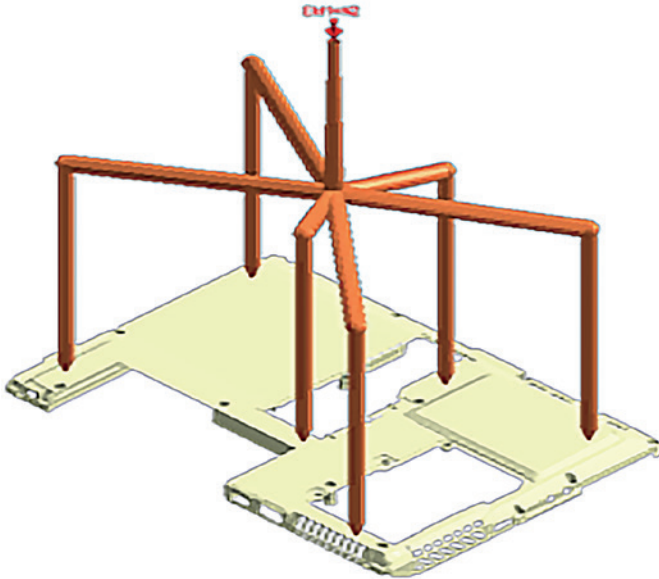


Figure 6.45 Product model

Figure 6.46(a) shows a single flow rate and Figure 6.46(b) illustrates a multi-step flow rate.

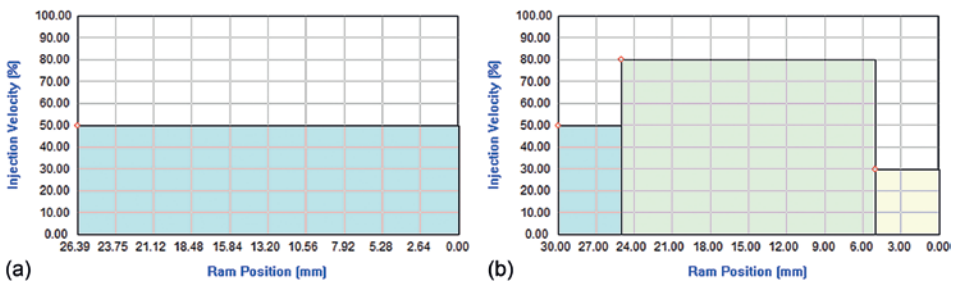


Figure 6.46 (a) Single flow rate and (b) multi-step flow rate

By examining the relationship of flow rate setting to injection pressure and shear rate at the gate as shown in Figure 6.47(a), where the red line denotes a single flow rate, while the blue line denotes a multi-step flow rate, it is found that a multi-step flow rate is able to reduce pressure loss effectively. Also in Figure 6.47(b), where the red line denotes a single flow rate, while the blue line denotes a multi-step flow rate, a multi-step setting is able to reduce the shear rate at the gate as well.

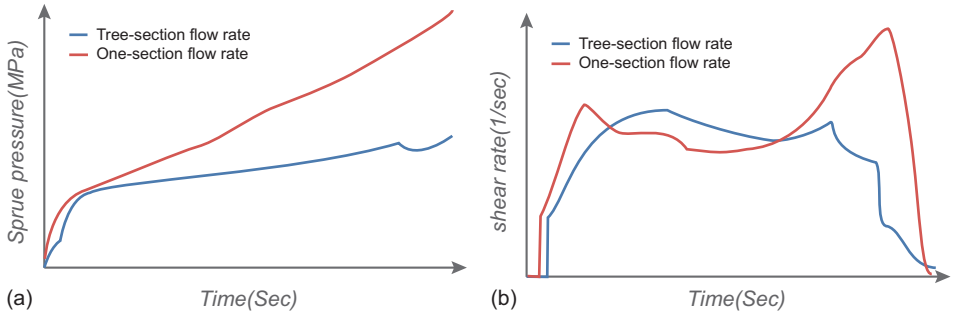


Figure 6.47 (a) Sprue pressure and (b) shear rate

■ 6.3 CAE Case Study

Following the discussions of this chapter and the corresponding CAE verification case, an exercise model, as illustrated in Figure 6.48, is provided in this section for readers to practice CAE application in runner and gate design.

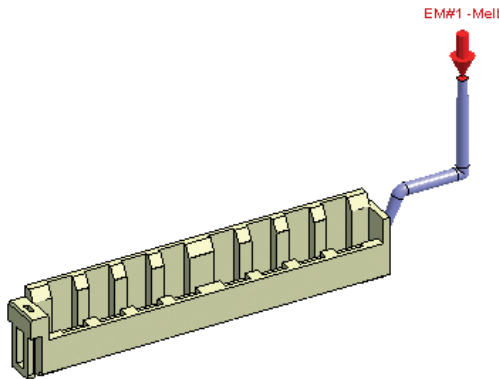


Figure 6.48 Case study sample

Please download the analysis files for CAE Case Study 6.3 from the following website:

<https://moldex3d.box.com/s/zr6fvc1vlhbi4ocx111jwd3wmxt4ooif>



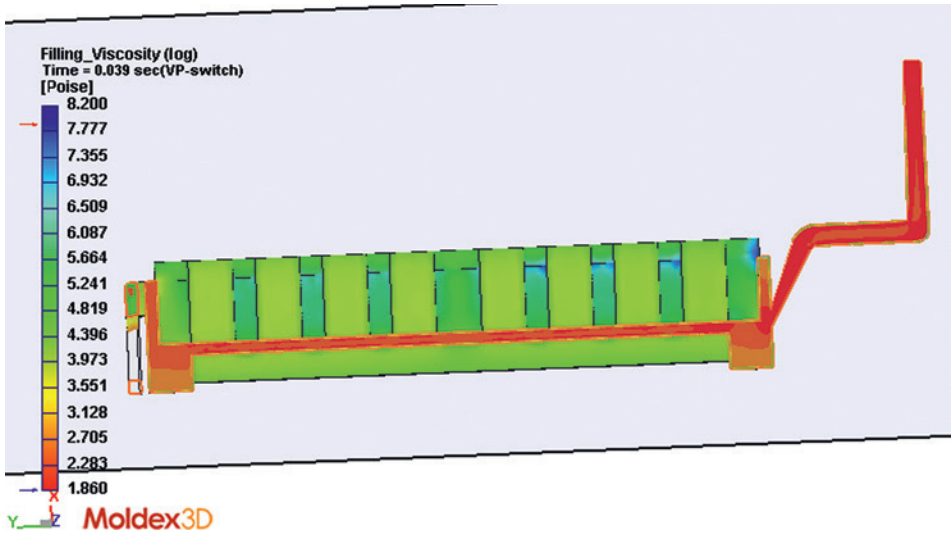
Then open the .m3j or .mvj file in Moldex3D and answer the questions below according to the analysis results.

Questions:

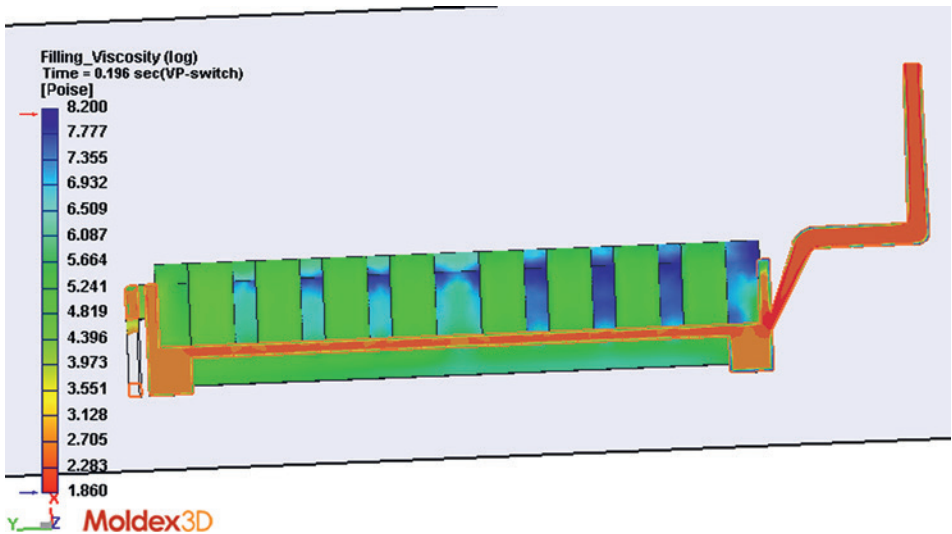
1. Pre-analysis of the model
 - a) What is the maximum L/t of the case? If taking PA6 as the material, does short shot occur? Why?
 - b) Where will be the filling ends and weld lines?
2. Comparison of different plastic materials
 - a) Run the simulations of flow analysis with “PA Ultramid 8202 BASF” and “PC+ABS CYCOLOY C7410 SABIC(GE)”. Why is the sprue pressure of PC+ABS much higher than that of PA? Try to explain the reasons with the comparison function of material wizard.
 - b) What makes the differences in the simulation results of viscosity and shear stress at EOF (end of filling) between PA and PC+ABS? Try to explain the reasons with respect to material properties.
 - c) Explain how the high-viscosity material affects the molding results, including molding processes and product quality.
3. Comparison of different process conditions: filling time
 - a) The default filling time is 0.1 sec. Compare the sprue pressure results for different filling times from 0.04 to 0.2 sec. Here we set a single flow rate profile. (Hint: check the XY-plots of sprue pressure curves.)
 - b) Figure 6.49 shows the internal viscosity results of filling time of 0.04 and 0.2 sec. Why does the viscosity distribution differ with the filling time? (Hint: check the temperature distribution.)
4. Comparison of different process conditions: flow rate
 - a) The default flow rate is three-segment profile. Compare the XY-plots of sprue pressure curves of different flow rates with single- and three-segment profiles.
 - b) Compare the shear rate distributions at the gate of different flow rates with single- and three-segment profiles (by clipping function).
5. Comparison of different process conditions: VP switch
 - a) The default VP switch is at 98% filling volume. Compare the XY-plots of sprue pressure and clamping force curves of different VP switch points at 90%, 98%, and 99% filling volume. Try to explain the reasons for the difference.
 - b) Compare the locations of weld line and welding temperatures. Try to explain the reasons for the difference.

6. Comparison of different wall thicknesses

- Compare the XY-plots of sprue pressure and try to explain the reasons for the difference.
- Try to catch the melt front time result with the set perspective of 90, 0, 90 on “view control panel” to show the filling difference caused by thickness change.
- Compare the shear stress distributions at EOF and try to explain what kind of bad influence to the part might be caused by changing thickness.



(a)



(b)

Figure 6.49 Internal viscosity results (by the clipping function with the plane of $z = 1$) at VP switch for the filling time of (a) 0.04 sec and (b) 0.2 sec

9.1.1 The Causes of Warpage

There are various reasons for warpage, including geometric factors such as part design, insert effect, process conditions including pressure and temperature, and material properties such as fibers and Pressure-Volume-Temperature (PVT) behavior. In order to resolve warpage, identifying the cause(s) is critical. Normally a fishbone diagram, as shown in Figure 9.5, is used to list all possible causes for warpage, which then can be compared with the real case to narrow down the source.

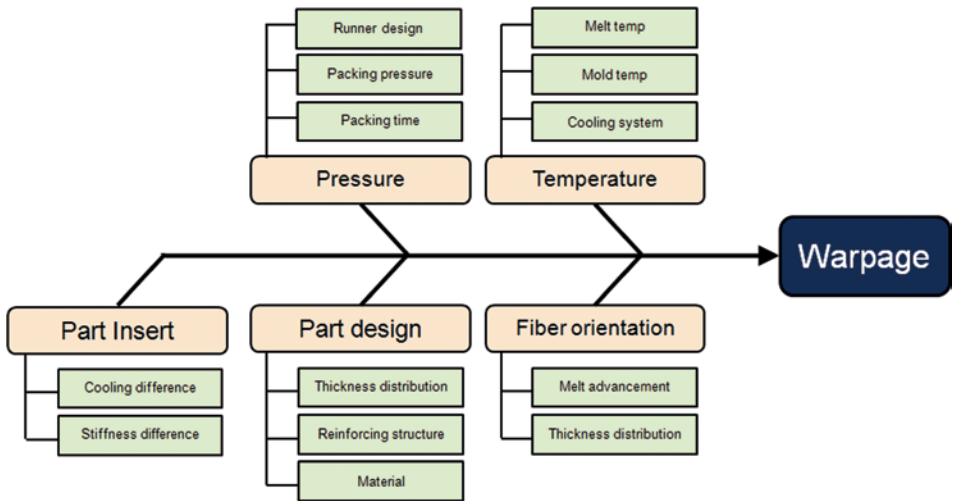


Figure 9.5 Fishbone diagram for warpage troubleshooting

1. Material

The plastic properties affecting shrinkage and warpage include plastic type, degree of crystallization (crystallization rate), and filler properties. Shrinkage behavior varies between different plastic types. For example, polyoxymethylene (POM) is a highly crystallized material and presents significant shrinkage after ejection. Polypropylene (PP), on the other hand, has a relatively minor shrinkage. Amorphous polymers such as poly(methyl methacrylate) (PMMA) have the lowest shrinkage rates. The crystallization rate is related to cooling. Nylon is a material with a low crystallization rate compared to the short injection filling time. The cooling is too fast for a high relative degree of crystallization, which leads to further shrinkage even after mold release. Fillers (inorganic substances) are basically rigid and do not shrink substantially, which makes them ideal for improving the mechanical properties and lowering the shrinkage of the polymer matrix. However, the induced viscosity increase in the melt poses challenges to processing with high filler content.

2. Part Design

Regarding the design of parts and molds, as heat tends to accumulate in the center area of the wall thickness, this area tends to shrink more after the packing pressure is released. The constantly dropping temperature would cause volumetric shrinkage in the original high-temperature areas. A single flat plate does not warp as the shrinkage on both sides is the same; however, warpage may occur if ribs are designed on one side. Usually, the ribs cause more shrinkage due to heat accumulation, such that the plate then bends toward the rib side. In some cases, inclusions such as glass fibers when properly aligned may reduce the rib-side shrinkage so that the warpage direction is opposite to the unfilled one. In the following sections, the mechanisms of how ribs, screw boss, and gussets affect warpage will be introduced.

Inserts are normally made of metal, which is stiffer than plastic, and act as reinforcements. Usually, they decrease the warpage. In some cases, an asymmetric shape of inserts may cause non-uniform shrinkage leading to warpage.

3. Mold Design

As for the mold design features, the gate location affects the packing effect in the part, and an irregular pressure distribution would lead to non-uniform shrinkage and cause warpage. How gates affect pressure distribution will be discussed later.

A good design of cooling channels effectively removes heat away from the part, and also homogenizes the temperature. Warpage is less significant if the temperature becomes uniform. But due to the spatial limitations of the mold (avoiding sliding blocks and ejection pins), the arrangement of cooling channels is often less than ideal. Also, the contact between the mold metal and mold mechanisms is unlike one block of material and thus does not conduct heat so well. On the other hand, some molds utilize high thermal conductivity metals such as beryllium copper to better transfer heat from the hot areas to the cooling system. This allows a shorter cycle time and provides a more uniform temperature distribution.

4. Process

Among all the molding process parameters, temperature and pressure are the most important ones to affect warpage because they relate directly to material shrinkage, i.e., PVT behavior. In addition, the faster the injection speed is, the higher the pressure becomes and so the temperature becomes more uniform, as the time it takes for a plastic material to flow from the gate to the end is shorter.

In the packing stage, the controllable parameters are packing pressure, packing time, multi-stage packing, cooling time, and cooling rate. These are all critical factors that affect shrinkage and warpage. During the filling, packing, and cooling stages of plastic molding, as the temperature and pressure keep changing and are

distributed non-uniformly, the density also varies with time and among different areas of the part, leading to non-uniform shrinkage eventually.

The injection molding process can be understood by the changing history of temperature and pressure, the most important causes for part warpage. As shown in Figure 9.6 and Table 9.1, the pressure rises in the filling stage from 1 to 4 along with the occurrence of high packing pressure from 2 to 3 and shear heating from 3 to 4. The cooling stage is from 4 to 5, in which the pressure also decreases. A dynamic process like this changes the density throughout the whole process and complicates the material shrinkage behavior.

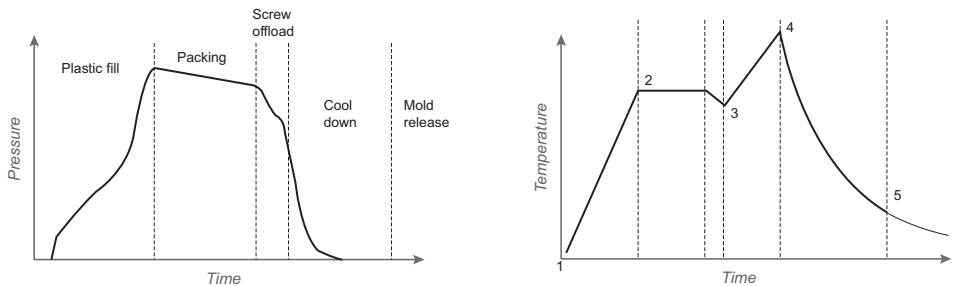


Figure 9.6 Pressure and temperature history of an injection molding process

Table 9.1 Stages of an Injection Molding Process

Stage (see Figure 9.6)	Description
1→2	Plastic enters the barrel and is heated up quickly
2→3	Plastic heats up until melted fully while maintains constant temperature
3	Plastic enters the screw to be heated up by a shear friction
3→4	Injection molding at high speed. Severe shear friction causes even higher temperature
4→5	Injection completes and the materials are cooled down through mold wall
5	Demolding

9.1.2 Material Effects

In addition to pressure, the molecular chain orientation also contributes to non-uniform shrinkage in the part. Both amorphous and semi-crystalline materials are stretched in the flow field when the temperature becomes higher than the phase-transition temperature including T_g or T_m (Figure 9.7 and Figure 9.8). The stretched chains tend to retract back to their most relaxed state with a globular conformation. If the material is frozen because of the fast cooling near the surface, the

strong tendency of the chain to retract causes a larger shrinkage along the flow direction than perpendicular to it. The difference of shear rate leads to a change of the orientation through the thickness. The shrinkage thus becomes anisotropic. If a flow is complex, the shrinkage will not be symmetric across the thickness direction. This will lead to unpredictable warpage for the part; hence, the first step to improving warpage is to simplify the flow. Materials with fibers show even more complex shrinkage behaviors along the direction perpendicular to flow compared to simple polymer chains, as the shrinkage of fibers is different to that of the resin. Warpage is even more complex when the cooling rate of a crystalline material differs, because the induced degree of crystallization and crystalline structure are different so the shrinkage distribution becomes even more unpredictable.

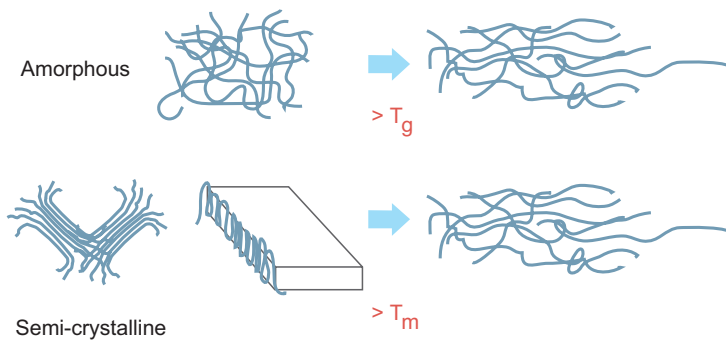


Figure 9.7 Amorphous and crystalline polymers

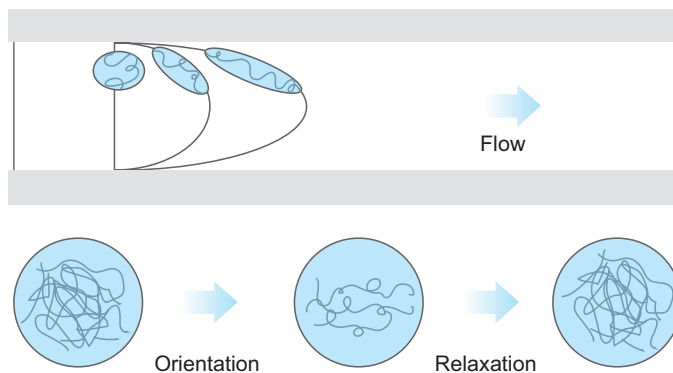


Figure 9.8 Molecular chain orientation caused by a shear flow of fountain flow

Since fibers cannot be stretched, they respond to shear flow by orientation along the flow direction. A simple shear flow results in a uniform orientation, but for fountain flow between the mold walls in injection molding, as shown in Figure 9.9

and Figure 9.10, fibers tend to align along the flow direction near the surface whereas they become perpendicular at the center of thickness area. This anisotropy leads to differential shrinkage between the layers of the part. If the orientation is unsymmetrical between the top and bottom shell layers, non-uniform shrinkage occurs and the part may start to warp.

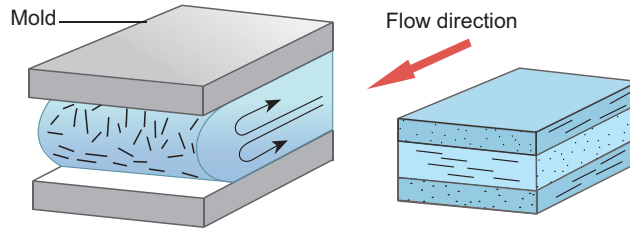


Figure 9.9 Fiber orientation caused by fountain flow

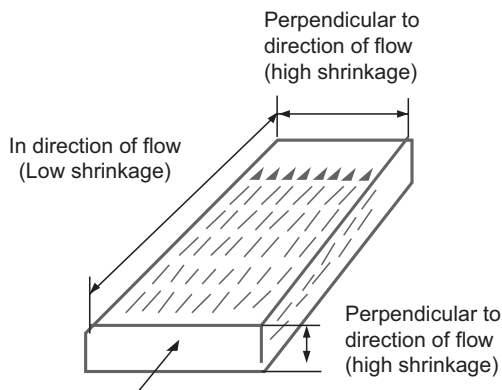


Figure 9.10 Fiber orientation effect on different part shrinkage parallel and perpendicular to the flow direction

Figure 9.11 shows different warpage behavior of an exemplary ribbed plaque caused by different flow directions for the ribs. When the melt enters the plaque parallel to the rib direction, the ribbed half shrinks less so the part shrinks downward. A flow perpendicular to the rib direction leads to an upward shrinkage instead.

Apart from the influence of the flow on the orientation of the molecular chains of the plastic material, the occurrence of warpage is also related to shrinkage behavior. A PVT diagram explains the shrinkage properties of a plastic (Figure 9.12; see Section 2.3.3 for more details). The crystalline material has a sharper transition caused by crystallization during cooling and its shrinkage ratio is higher compared to an amorphous material.

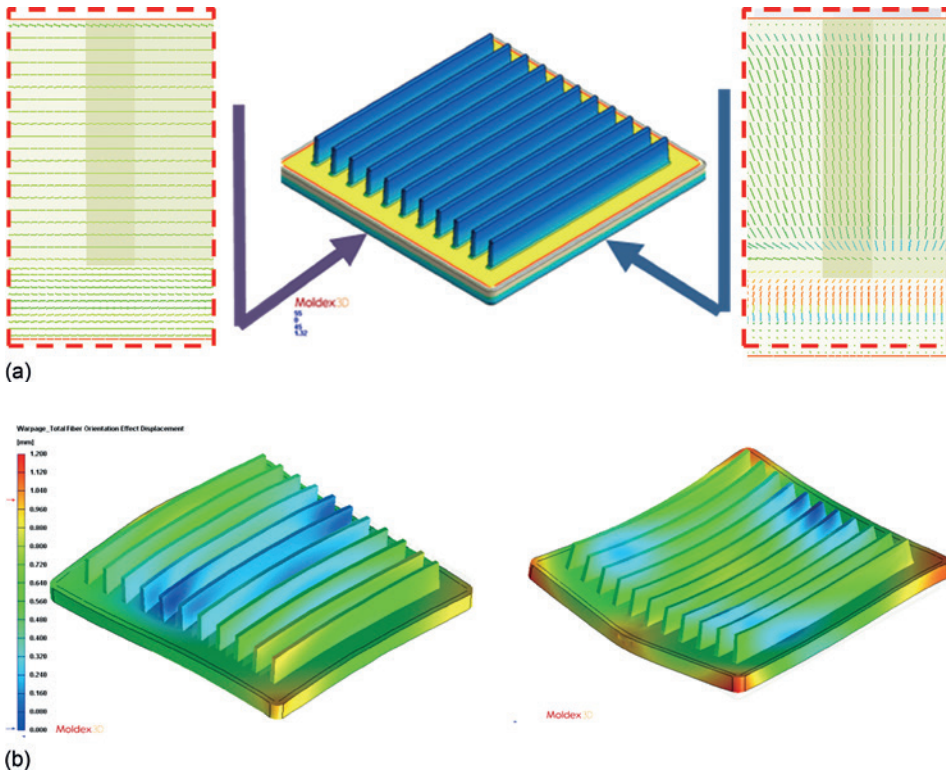


Figure 9.11 (a) Fiber orientation results in the rib section of a plaque with multiple fins. Two gate locations lead to either parallel flow or cross flow inside the fin. (b) The different fiber orientation of fin area leads to different warpage patterns

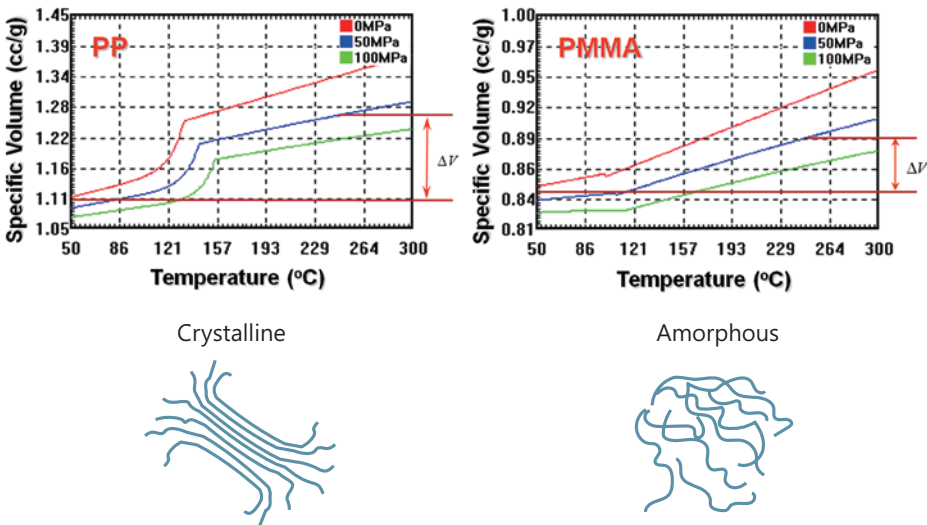


Figure 9.12 PVT diagrams of crystalline and amorphous plastic materials

9.1.3 Geometrical Effects

In Chapter 3 of this book ("Part and Mold Design"), we have introduced part design principles that focus on the part geometrical effect on the flow of plastic as well as the orientation of molecular chains and fibers, and their result on the anisotropic shrinkage. More details about geometrical effects on warpage are discussed here. Since thickness changes in a part are inevitable, the wall thickness needs to be made as uniform as possible for continuous and gradual change. As shown in Figure 9.13, a smooth transition reduces the internal stress caused by a discontinuity of volume shrinkage.

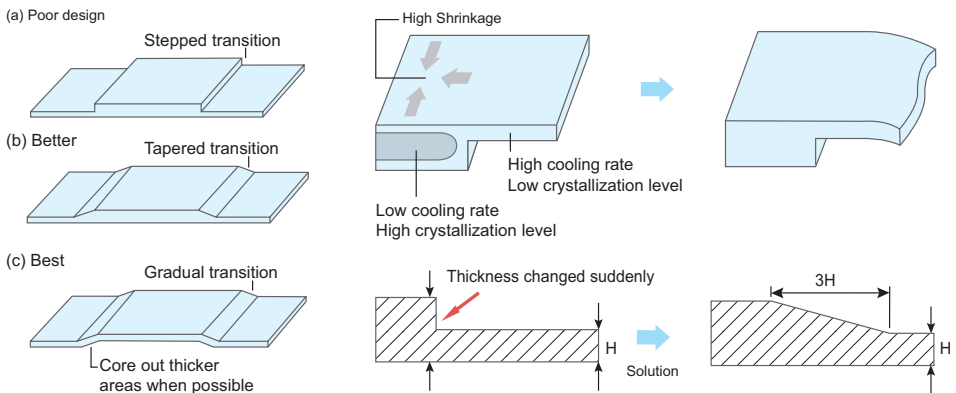


Figure 9.13 Effect of thickness on warpage: a gradual change of thickness is preferred in preventing warpage

As cooling is slower for thicker parts, for crystalline plastics, a slower cooling would generate a higher degree of crystallization in a larger area, which results in higher shrinkage. For thin parts, a high flow rate and the shear effect lead to a more significant orientation along the flow direction, which results in a higher internal stress and more severe warpage.

For a flat plate or box-shaped product, features such as ribs and bosses are often used to reinforce the part. But, as shown in Figure 9.14, ribs also tend to cause unpredictable results of warpage. If the spacing between the ribs is too small to allow enough cooling channels to pass through, the ribbed area would accumulate heat and induce warpage. For mold makers, it is thus preferred to evaluate the warpage level from a molding simulation based on the materials used, the gating location, and the design of the cooling channels.

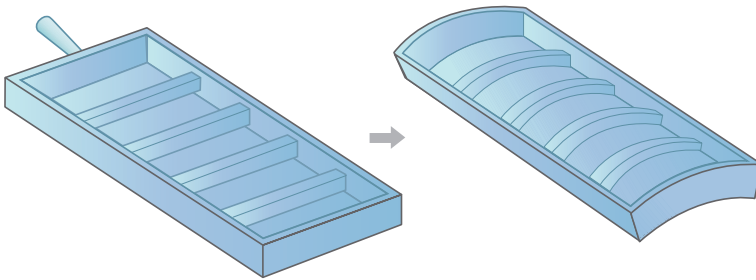


Figure 9.14 Effect of reinforcing rib on warpage: necessary core-out or cooling should be performed to prevent warpage

Cutting ribs into sections is one way of easing warpage. As shown in the top design of Figure 9.15, the bottom of the part is thicker, thus having a higher shrinkage. The thinner ribs do not shrink as much as the bottom so a concave shape is the result. Below are improvements that can eliminate this warpage, including cutting off the consecutive plane on the upper part, which restrains the shrinkage, or the rib can be designed more symmetrically so that the warpage would not be significant while the stiffness can still be maintained.

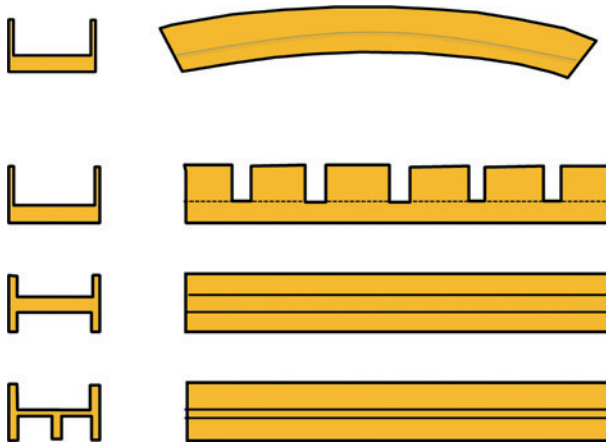


Figure 9.15 Top: uneven thickness distribution leads to warpage; below: improved rib designs to eliminate warpage

When fiber-reinforced plastics encounter a change in thickness, a strong elongational flow orients the fibers as shown in Figure 9.16. The fibers orient better as the flow passes from thick to thin areas as in a converging flow. The effect of this stretching in changing the fiber orientations is stronger compared to shear flow. This is another source of inducing anisotropy into the part apart from shear flow. Parts gated at the center have a strong diverging flow at the beginning of filling. This often leads to a bowl- or dome-shaped warpage.

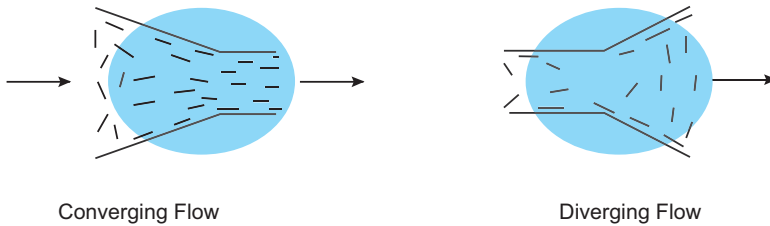


Figure 9.16 Comparison of fiber orientation during converging and diverging flow

9.1.4 Process Condition Effects

Temperature and pressure are the main causes that induce shrinkage. Six factors can be defined in comparison to site conditions: melt temperature, mold temperature, injection speed, packing pressure, packing time, and cooling rate. It is very difficult to test these six factors by trial and error; therefore, we should first understand how they affect shrinkage.

Normally a reduction of shrinkage can be achieved by lowering the melt temperature, increasing the packing pressure, and prolonging the packing time, whereas the mold temperature and injection speed have limited effect on shrinkage. In a cooling process, the mold temperature would not play a critical role unless a material of slow crystallization rate is used, or the mold temperature is too low causing early cooling and insufficient crystallization. The injection speed affects temperature and pressure indirectly. Normally the dynamic range of the injection speed of the machine is not wide, and so is the allowed injection speed range for the part. Therefore, the injection speed, melt temperature, and pressure can all be managed within an adjustable range.

The molding parameters of filling should control the rheological behavior of the plastic material: how much time it needs for filling, and how much pressure should be used for injection. If the injection pressure cannot be evenly distributed in the part, a significant difference in volumetric shrinkage will occur despite applying an excessively high pressure. A localized high injection pressure easily turns into residual stress which deteriorates the part. An ideal injection process ensures that enough material enters the cavity and that the subsequent packing pressure compensates for the shrinkage caused by material cooling. Refer to Chapter 6 for details regarding the effect of pressure on product shrinkage.

Regarding temperature, the shrinkage grows as the temperature of the melt increases. If the melt temperature is too low, the gate will freeze too early rendering the subsequent packing useless. The mold temperature can further be controlled independently via two mold temperature controllers on the two sides of the part

separately. This allows warpage to be actively controlled by manipulation of the part shrinkage on both sides. As shown in Figure 9.17, generally the cooling efficiency of the mold core is poor and the shrinkage is high. To solve the problem, the temperature of the mold core can be lowered to ease the shrinkage, while increasing the temperature of the cavity side for better surface quality.

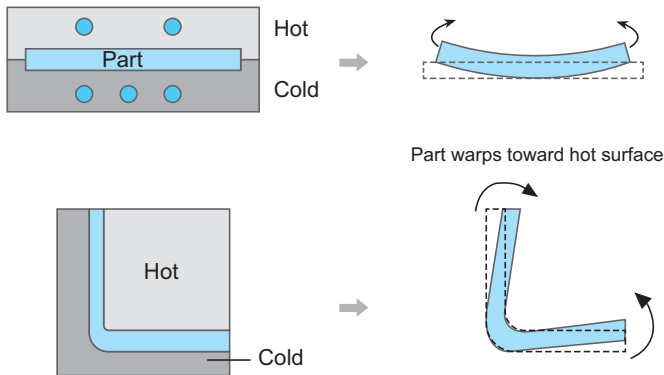


Figure 9.17 Part warpage tendency due to global or localized mold temperature difference

9.1.5 Criteria of CAE Warp Analysis

According to the above principles, CAE can be used for warpage analysis to assess (1) uniform cooling and mold temperature distribution, (2) effective packing before gate freezes, (3) shrinkage due to part geometry, (4) fiber orientation effects on warp, and (5) displacement/flatness prediction:

1. Uniform Cooling and Mold Temperature Distribution

As the cooling channel suitable for both mold cores and mold cavities is different, the induced difference in cooling efficiency would result in distinct shrinkage. It is hard to install a cooling channel at the corner of the mold core, and thus the shrinkage becomes higher. It is thus often seen in box-like parts that the shrinkage at corners is more serious, showing a concave condition around the corners.

In the Moldex3D software, the “Mold temperature difference” function can be used to visualize the difference in mold temperature. Generally, a difference is preferred but which shall maintain a uniform and constant value. The cross-sectional view of the mold temperature could help the user find the problematic hot spot. As shown in Figure 9.18(a), the center of this exemplary fan part shows high temperature even after cooling, which results in notable warpage at the blades (Figure 9.18(b)). If cooling channels can be applied to this side, the warpage can be reduced.

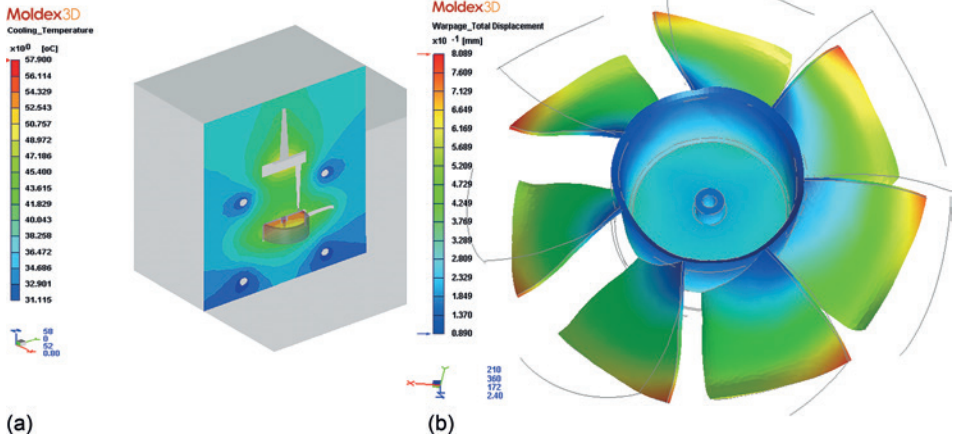


Figure 9.18 (a) Mold temperature cross-section CAE results showing heat accumulation on the core side, and (b) warpage of the part

2. Effective Packing before Gate Freezes

Gate freezing has a key effect on the success of packing. If the gate seals due to cooling, even a higher packing pressure will not contribute to the effectiveness of packing. Therefore, whether the gate is sealed or not should be particularly observed in a simulation analysis. It can be seen from the temperature distribution chart shown in Figure 9.19 that the high-temperature area (green) locates around the middle of the runner, while the temperature is lower at the gate and inside the part, which means that the pressure cannot be effectively transferred into the part if the packing is done from the right side (Figure 9.19).

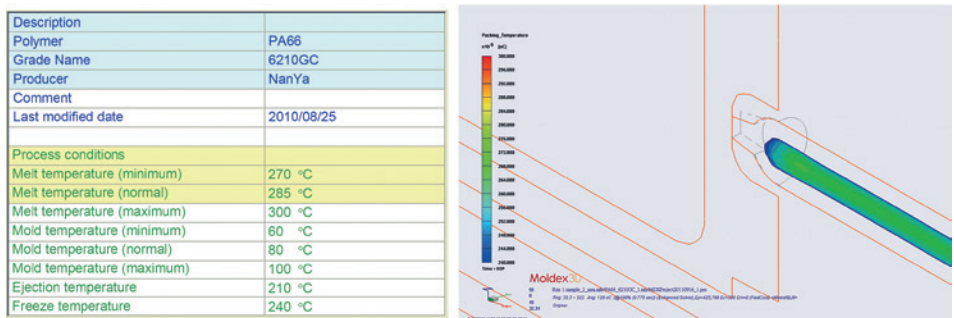


Figure 9.19 Effective packing before gate freezes

3. Shrinkage Due to Part Geometry

Shrinkage difference due to the thickness and geometry characteristics of a part can also affect how a molded part warps. Figure 9.20 shows a slicing of volumetric shrinkage extracted from Moldex3D for a connector case, where its thickness is distributed unevenly. Thicker sections have larger volumetric shrinkage than thinner regions, because heat accumulates more easily in the thicker section, as it is more difficult for cooling to reach the middle area. Because of the uneven thickness distribution, the volumetric shrinkage varies. Therefore, a well-considered part design is an essential point to prevent product warpage.

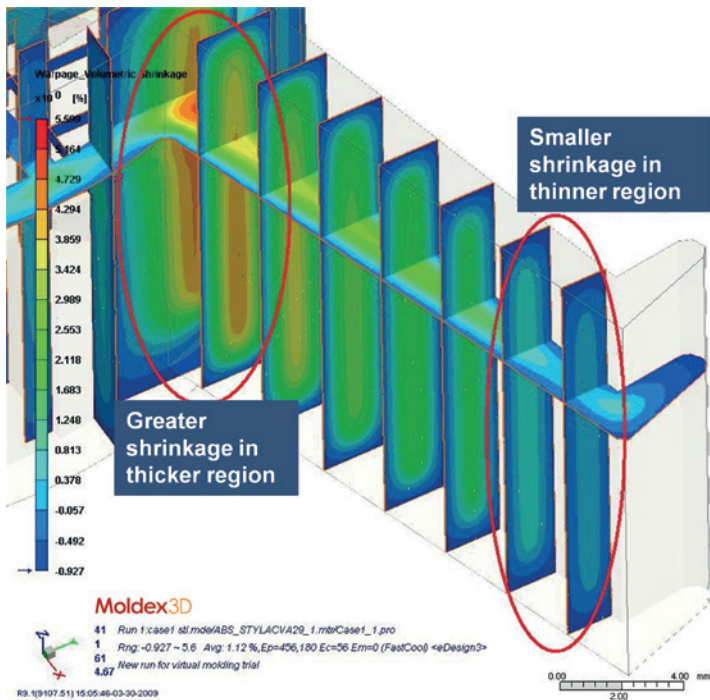


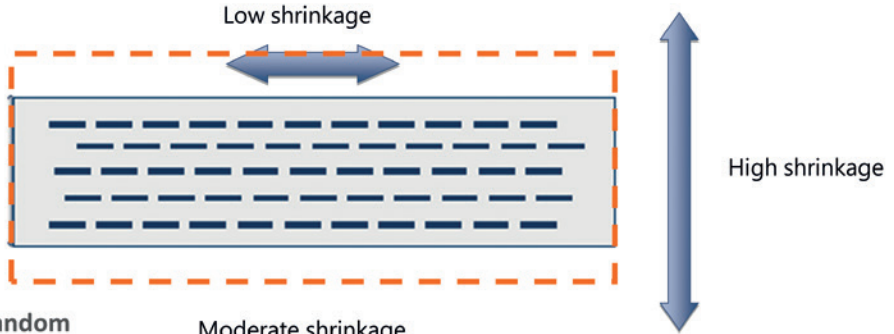
Figure 9.20 Shrinkage difference: thickness and geometry characteristics

4. Fiber Orientation Effects on Warp

As fiber orientation due to flowing creates anisotropic properties in the material, anisotropic shrinkage and warpage are thus generated. The fiber orientation effect can be verified by CAE. Fibers tend to align in the flow (forward) direction, especially in the area close to the mold wall. Shrinkage along the forward direction of fiber orientation is relatively smaller. If fibers are aligned well, the shrinkage along the long axis (forward) becomes smaller; if not, shrinkage would be similar in both directions. A randomized fiber orientation has a more uniform shrinkage along

and cross-flow direction compared to the aligned one with an anisotropic shrinkage, as shown in Figure 9.21.

> **Highly oriented**



> **Random**

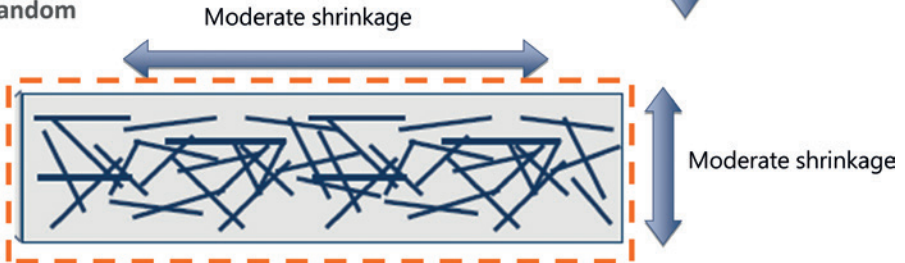


Figure 9.21 Highly-oriented and randomized fiber orientation, and corresponding shrinkage

Figure 9.22 shows a poor orientation of the fibers on the top half of the part, leading to isotropic shrinkage, but on the bottom part the fibers are highly oriented giving rise to strong anisotropic shrinkage. However, as the shrinkage along the direction of flow is smaller, we can see as a final result that the shrinkage on the bottom part is small, whereas that on the top half is large, causing the part to warp upward.

Index

A

advanced hot runner (AHR) 335
air trap 11, 184, 296
amorphous 20, 38, 278
anisotropic 442, 452, 463
anisotropic rotary diffusion (ARD) model 308
anisotropic rotary diffusion (ARD) tensor 312
anisotropic tensor 431
Arrhenius equation 47
aspect ratio 309, 315
autocatalytic kinetic model 51
Avrami equation 48

B

back pressure 94, 101, 105
baffle 247
ball grid array (BGA) 479
barrel 6
bi-injection molding 359, 361
bilaminate 502
Bingham fluid 24
black line 435
blow-through 385
boss 61, 69
boundary layer mesh (BLM) 154
breakthrough 362, 366
brown part 427
bubbler 247
burn mark 12

C

carbon fiber 466
Carreau-Yasuda model 28
cashew gate 76, 215
Castro-Macosko model 52
cell growth model 407
cell nucleation model 408
ceramic injection molding (CIM) 425
chamfer angle 55, 60
chemical foaming 401, 417
chemorheology model 52
chip packaging 476
chip-substrate packaging 478
chisel gate 214
co-injection molding 358, 363
compounding 426
computational fluid dynamics (CFD) 237, 258
conformal cooling 250, 258
continuity equation 140
continuum surface force 486
control volume 139
convected Jeffrey model 32
conversion 457, 462
coolant 238, 249
coolant flow rate 119
cooling efficiency 249, 257
cooling stage 87, 98, 119
cooling temperature 101
cooling time 55, 97, 114, 252
Couette flow 431
cross-link 20, 50
crystalline 20, 38, 279

crystallinity 21, 47
curing 50
curing degree 486
curvilinear flow 431

D

Darcy's law 452
degree of cure 52
delamination 12
design for manufacture (DFM) 124
design of experiment (DOE) 290
diaphragm gate 213
die swell 30
differential scanning calorimetry (DSC)
36
dilatant fluid 24
disk gate 213
draft angle 61
dry spot 449
Dual In-line Package (DIP) 479

E

edge effect 450, 458
edge gate 77, 211, 327
ejection temperature 254, 92
ejector 76
elastic modulus 32, 47
elastic recoil 31
energy equation 140
equation of state 39
extrudate swell 30

F

fan gate 76, 212
fan-in 478
fan-out 478
feed 88, 106
fiber 276, 279
fiber orientation 76, 304, 307, 308, 314,
317
fiber-reinforced polymer (FRP) 442
fillet 60

filling stage 87, 96, 111, 115
filling time 110, 114, 164
film gate 212
fingering effect 387, 397
finite difference method (FDM) 141
finite element method (FEM) 147
finite volume method (FVM) 144
fish eye 12
flash 10, 92, 168, 177
flatness 126
flip chip bonding 477
flow balance 203, 218, 328
flow consistency index 28
flow imbalance 218, 223, 231, 334, 366
flow length 58, 185
flow length/wall thickness ratio 58, 126,
184
flow mark 13, 168
flow rate 166, 196
fluid-assisted injection molding 381
fluid-structure interaction (FSI) 489, 499
foaming with counter pressure 404
Folgar-Tucker diffusion model 310
fountain flow 362
frame level packaging 479
frozen layer 160, 184
full shot overflow method 380
full shot pushback method 381

G

gas-assisted injection molding (GAIM)
377
gate sealing 216
Giesekus model 33
glass transition 27, 35, 47
glassy region 45
granulation 426

H

heat capacity 35
heat flux 43
heating coil 330, 339
heat transfer coefficient 44

hesitation 14, 184
hesitation mark 386
hollowed core ratio 378, 389
hopper 3
hot runner system 325, 335
hot spot 255
hot-tip gate 327
hybrid mesh 226

I

impregnation 444, 449, 470
improved ARD and retarding principal
rate (iARD-RPR) model 308, 314
injection pressure 95, 111
injection velocity 110
insert molding 357
integrated circuit (IC) 475
intramolecular force 20
isotropic 463
isotropic rotary diffusion 308

J

Jeffery's hydrodynamic model 308
jetting 14, 72, 168, 208

K

knock-out pin gate 214

L

laminar flow 249
Land Grid Array (LGA) 479
lapped gate 211
lay-up 445, 462
Leaded/Leadless Chip Carrier (LCC)
479
lead frame 476, 489
liquid composite molding (LCM) 443
long fiber reinforced thermoplastic
(LFRT) 304

M

manifold 328
mat 444
Maxwell model 32, 47
melt fracture 31, 168
melt front area (MFA) 166
melting core 218
melt temperature 92
metal insert 290
metering stroke 94, 107
MFR (melt flow rate) 92
microcellular foam 402, 417
modified Cross model 28
modified Tait model 40
modified White-Metzner model 33
mold clamping 6, 87
mold design 71
molded underfill (MUF) 489
molding cycle 87, 115
molding instability 133
molding window 93
mold temperature 92, 120
momentum equation 140
multi-cavity system 220
multi-component molding (MCM) 357
multi-die stacking 495

N

Newtonian fluid 22, 32
non-Newtonian fluid 21
nozzle 87, 108
nozzle tip 327

O

ON/OFF control 331
over-molding 357

P

package-in-package (PiP) 495
packing pressure 89, 101
packing stage 87, 115

packing time 101, 118
paddle shift 487, 499
particle volume fraction 430
permeability 452, 467
Phan-Tien and Tanner (PTT) model 34
PID control 332
pin gate 76, 214
Pin Grid Array (PGA) 479
pin movement control 349
pin through hole 478
plasticizing stage 87
plastics 29
porosity 452
powder injection molding (PIM) 425
preform 447, 454, 466
Pressure-Volume-Temperature-Cure (PVT-C) model 488
Pressure-Volume-Temperature (PVT) 276, 290
primary fluid penetration 379

Q

Quad Flat No-leads (QFN) 479
Quad Flat Package (QFP) 479

R

race-track 127, 184, 185
reduced strain closure (RSC) model 308
reflow soldering 479
relaxation modulus 46, 488
relaxation time 32, 46
reptation 24
resin transfer molding (RTM) 441
Reynolds number 83, 249, 259
rib 61
ring gate 213

S

secondary penetration 397
Seemann composites resin infusion molding process (SCRIMP) 448

sequential multiple-shot molding 357
shape factor 309, 315
shark skin 31
shear layer 160
shear rate 22
shear stress 22
shear-thinning 162
shelf level packaging 479
short fiber reinforced thermoplastic (SFRT) 304
short shot 9
side gate 211
sink mark 11
solder bump 477
specific volume 39
Spencer-Gilmore-C model 41
Spencer-Gilmore model 40
splays 14
spoke gate 213
sprue dimension 204
sprue gate 77
stress mark 13
submarine gate 214
suck back 105
supercritical fluid (SCF) 402
surface mounting 478
System-in-a-Package (SiP) 480, 495
System-on-Chip (SoC) 479

T

Tait model 40
tape-automated bonding 476
thermal conductivity 43
thermal pin 248
thermal sprue gate 327
thermoplastics 20
thermoset 20
Thin Small Outline Package (TSOP) 479
transfer molding 480
tubeless siphon 30
tunnel gate 76
turbulent flow 249

U

U-curve theory 165
underfill 480
upper convected Maxwell model 32

V

vacuum-assisted resin transfer molding (VARTM) 448
valve gate 77, 215, 327, 350
venting 65, 84
viscoelastic flow 33
viscoelastic fluid 29, 47
viscoelasticity 29, 45
viscosity 22
void 11
void trapping 490
VP switch 115, 175

W

wafer-level chip scale packaging (WLCSP) 478
wall thickness 55
warp 9, 10
water-assisted injection molding (WAIM) 377
wave soldering 479
welding angle 74
weld line 15
White-Metzner model 33
wire bonding 476
wire sweep 486
wire sweep index (WSI) 493
WLF Equation 27
woven 444

Y

yield stress 29